



Cite this: DOI: 10.1039/c8nj05932b

Selective hydrogenation of nitroarenes to amines by ligand-assisted Pd nanoparticles: influence of donor ligands on catalytic activity†

Gauravjyoti D. Kalita,^a Podma P. Sarmah,^a Pallab Kr. Saikia,^b Lakshi Saikia^b and Pankaj Das^{*a}

Ligand-assisted synthesis of metal nanoparticles has advanced significantly; however, the influence of donor groups on the catalytic performances of such heterogeneous systems has not been systematically explored. Here, we have synthesized and characterized three ligand-based silica-supported palladium nanocatalysts via an impregnation-reduction method through anchorage of palladium onto silica gel functionalized with amine, phosphine and thiol. TEM images of the amine- and phosphine-based materials showed formation of uniformly distributed palladium nanoparticles (Pd NPs) with fine particle sizes, whereas the thiol-based material showed formation of palladium nanowires (Pd NWs) of irregular sizes. To investigate the influence of the donor ligands, selective hydrogenation of 4-chloronitrobenzene (4-CNB) to 4-chloroaniline (4-CAN) was carried out. Under similar experimental conditions, the catalytic activity decreased in the order of phosphine > amine > thiol. A maximum yield of 98% and selectivity of 100% was achieved with the phosphine-based catalyst using molecular hydrogen as a reducing agent. A diverse range of nitroarenes were efficiently converted to their corresponding amines.

Received 22nd November 2018,
Accepted 3rd February 2019

DOI: 10.1039/c8nj05932b

rsc.li/njc

Introduction

Over the past few decades, the selective hydrogenation of nitroarenes to amines has become a subject of apex priority both in industrial and academic domains. Among various amines, chloroanilines (CANs) have received particular attention because of their ardent necessity as intermediates in pharmaceuticals, dyes, pigments and fine chemical industries.^{1–5} Until now, the most widely acceptable protocol for large-scale production of CANs is the Béchamp's process which involves Fe-promoted stoichiometric reduction of nitro-compounds in acidic media.^{6–8} However, from economic and environmental perspectives, this protocol is no longer viable as it produces a significant amount of toxic waste apart from low selectivity and poor yield. In recent years, liquid-phase catalytic hydrogenation employing noble metals like Pt, Pd, Rh, Ru, *etc.* has emerged as a suitable alternative to the Béchamp's process.^{9,10} Although significant advancements have been made in terms of waste minimization and yield increment, the hydrogenation of 4-CNB to the corresponding 4-CAN is always accompanied by hydrodechlorination

as the major side reaction resulting in a decrease in selectivity of 4-CAN.^{11,12} To improve the product selectivity, many attempts have been made which includes tuning the steric and electronic properties of the ancillary ligands in homogeneous catalysts,^{13,14} controlling the sizes and shapes in the case of metal nanocatalysts^{15–19} or engineering surface properties in the case of supported heterogeneous catalysts;^{20–27} however, the side reaction of hydrodechlorination could not be fully circumvented. Moreover, the majority of the above systems use reducing agents, like hydrazine derivatives,¹⁵ sodium borohydrides,^{28–30} hydrosilanes³¹ *etc.*, that have serious environmental concerns.³² Thus, recently much attention has been given towards designing more promising recyclable hydrogenation catalysts that ensure selective reduction of 4-CNB keeping intact the C–Cl bond using molecular hydrogen as a reducing agent. Nevertheless, there exist a few successful examples of such catalysts, like Ru/Fe₃O₄,³³ Ru/CNT,¹⁶ Au/ZrO₂,¹⁹ Pd/N-CMK-3³² *etc.* Although, a few of the aforementioned systems seem promising, tedious synthetic protocols,³⁴ high metal loading,³⁵ drastic reaction conditions,³⁶ *etc.* are some of the limiting factors for their industrial scale applications. Hence, development of new catalytic systems that induce efficient reduction of nitroarenes using molecular H₂ as reducing agent under mild condition is still more appealing.

It is noteworthy to mention that ligand-assisted synthesis of metal nanoparticles (MNPs) has received immense importance because of their potential applications in catalysis.^{34–39} Compared to

^a Department of Chemistry, Dibrugarh University, Dibrugarh, Assam, 786004, India.
E-mail: pankajdas@dibru.ac.in

^b Materials Sciences and Technology Division, CSIR-North East Institute of Science and Technology, Jorhat, Assam, 785006, India

† Electronic supplementary information (ESI) available. See DOI: 10.1039/c8nj05932b

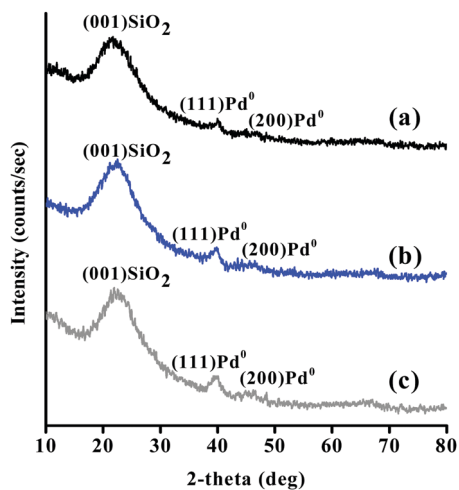


Fig. 3 Powder X-ray diffraction patterns for (a) Pd-AP@SiO₂, (b) Pd-DPPE@SiO₂ and (c) Pd-MP@SiO₂ materials.

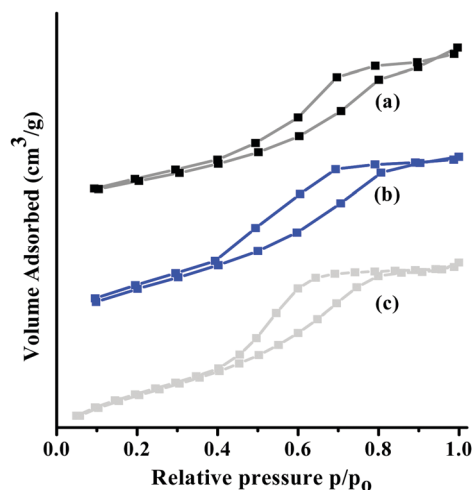


Fig. 4 N₂-sorption isotherms for the Pd NP incorporated silica-based materials: (a) Pd-DPPE@SiO₂, (b) Pd-AP@SiO₂ and (c) Pd-MP@SiO₂.

fcc Pd NPs. A broad peak corresponding to the silica phase was observed at around $2\theta = 22.4^\circ$ for all the materials which is consistent with the parent support. This indicates that the mesoporous structure of the silica matrix remained intact upon Pd loading. The N₂ adsorption-desorption isotherms were measured for the materials at 77 K and the physical parameters were compared with those for the parent supports. The N₂-sorption measurements of the functionalized silica materials showed an isotherm with the characteristic type IV hysteresis loop for mesoporous materials. A prominent decrease in the surface area compared to the neat supports was observed (Table 1). This decrease in surface area may be attributed to the generation of Pd NPs/NWs within the pores of the silica matrices (Fig. 4).

The binding energies of the Pd 3d state for all the synthesized materials are shown in the XPS spectrum [Fig. 5(a)–(c)]. The bands observed at 335.2 and 340.8 eV for Pd-DPPE@SiO₂ and 335.5 and 341.1 eV for Pd-MP@SiO₂ are attributed to Pd 3d_{5/2} and 3d_{3/2} states, respectively, coherent with the value for Pd(0) species.^{43,47} This indicates the complete reduction of Pd(+2) to Pd(0). A slight increase in the binding energies (+0.1 eV for Pd-DPPE@SiO₂ and +0.4 eV for Pd-MP@SiO₂) from that of metallic Pd was observed. This may be attributed to the interaction of P- and S-donor atoms on the ligand-functionalized silica matrices which induces a small positive charge on the metal surface. On the other hand, for Pd-AP@SiO₂ [Fig. 5(c)], the bands at

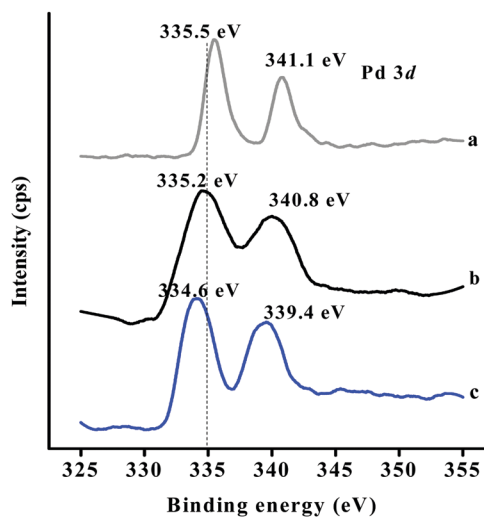


Fig. 5 XPS spectra for the materials: (a) Pd-MP@SiO₂, (b) Pd-DPPE@SiO₂ and (c) Pd-AP@SiO₂ showing Pd 3d_{5/2} and 3d_{3/2} states.

334.6 and 339.4 eV exhibit a slight decrease in BE (−0.5 eV), which is due to the strong sigma donor capability of N-donor sites inducing a small negative charge on the metal surface.

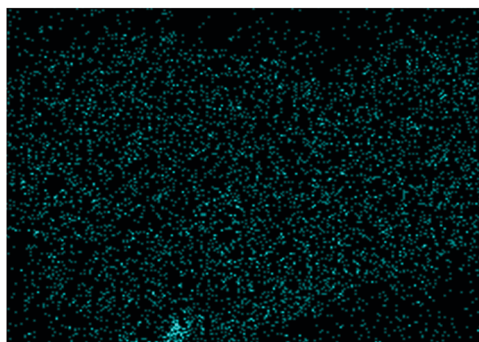
To study the thermal behavior of the synthesized materials thermogravimetric analysis was carried out under N₂ atmosphere. The samples were observed to be stable up to 350 °C. With further increase in temperature, significant loss of weight corresponding to the decomposition of alkylsilane moieties (ligand part) of the functionalized silica was observed [Fig. S3 (ESI[†])]. The total organic contents were also measured from the TGA analysis and were found to be 8, 9 and 5 wt% for the thiol, amine and phosphine-functionalized samples, respectively. The elemental dot mapping images for Pd-DPPE@SiO₂ invariably demonstrated a uniform distribution of Pd throughout the support matrix as determined from Fig. 6. The amount of Pd present on the synthesized materials was estimated by ICP-AES analysis and found to be 0.84, 0.52 and 0.51 wt% for Pd-DPPE@SiO₂,

Table 1 A comparative study of the surface area, pore volume and metal content of the Pd NPs with their respective neat supports

Sample	S_{BET}^a [m ² g ^{−1}]	Pore volume ^b [cc g ^{−1}]	Pd ^c [wt/wt%]
DPPE@SiO ₂	500.9	0.476	—
AP@SiO ₂	550.3	0.882	—
MP@SiO ₂	500.0	0.634	—
Pd-DPPE@SiO ₂	411.3	0.263	0.84
Pd-AP@SiO ₂	482.0	0.823	0.52
Pd-MP@SiO ₂	231.7	0.445	0.51

^a BET surface area. ^b Total pore volume was measured at $P/P_0 = 0.98$.

^c Metal content of the Pd NPs as measured from ICP-AES analysis.



Pd La1

Fig. 6 EDS elemental mapping analysis for palladium in the as prepared Pd-DPPE@SiO₂ material.

Pd-AP@SiO₂ and Pd-MP@SiO₂ respectively (Table 1). This indicates that the phosphine-functionalized ligands stabilize the Pd NPs more efficiently compared to the amine and thiol-functionalized counterparts.

Catalytic activity

To explore the catalytic activities of the Pd NPs, hydrogenation of nitroarenes to their corresponding amines was carried out with 4-CNB as the model substrate using ethanol as solvent. Initial screening reveals that under similar experimental conditions, among the three catalysts, Pd-DPPE@SiO₂ (Pd = 0.84 wt%) exhibited superior catalytic performance, and the results are summarized in Table 2. It is almost established that MNPs with smaller particle sizes usually exhibit better catalytic performance due to their preferentially exposed surface area; however, in the present study, even though the particle sizes are more or less similar, the materials Pd-DPPE@SiO₂ and Pd-AP@SiO₂ showed contrasting catalytic activities. Higher conversion and selectivity were observed in the case of the former compared to the latter (Table 2, entries 1 vs. 2). This result clearly suggests that the donor groups have some implications on catalytic performance. The efficiency order of the catalysts follows the trend: Pd-DPPE@SiO₂ > Pd-AP@SiO₂ > Pd-MP@SiO₂. Given the distinct selectivity response for 4-CAN, Pd-DPPE@SiO₂ was chosen for further comprehensive catalyst optimization protocols.

To further optimize the reaction conditions such as reaction time, temperature, metal loading, catalyst:substrate ratio, hydrogen pressure, *etc.* for better catalytic performance, a number of runs were performed with Pd-DPPE@SiO₂ (Table 3). It was

Table 2 Hydrogenation of 4-CNB to 4-CAN with Pd NPs as catalysts under liquid phase conditions^a

Entry	Nanocatalyst	Catalyst amount ^b (mg)	Conv. ^c [%]	Sel. ^c [%]
1	Pd-DPPE@SiO ₂	50	98	90
2	Pd-AP@SiO ₂	81	66	35
3	Pd-MP@SiO ₂	82	Trace	100

^a Reaction conditions: solvent (4.5 mL), H₂ pressure (10 bar), 400 rpm, and 50 °C, 2 h. ^b Varying amounts of catalyst were added to ensure equal Pd content on the support (0.0039 mmol). ^c Determined by GC analysis. [Conv. = conversion, and Sel. = selectivity].

Table 3 Hydrogenation of 4-CNB to 4-CAN with Pd-DPPE@SiO₂ as the catalyst under liquid phase conditions^a

Entry	Pd cont. ^b (wt%)	Substrate (mmol)	Time (h)	Conv. ^c [%]	Sel. ^c [%]
1	0.84	0.5	0.5	90	100
2	0.84	0.5	1	95	83
3	0.84	0.5	2	98	90
4	0.84	1	2	86	83
5	1.65	0.5	0.5	80	73

^a Reaction conditions: catalyst (50 mg), solvent (4.5 mL), H₂ pressure (10 bar), 400 rpm, and 50 °C. ^b Pd loading on support in wt% determined by ICP-AES analysis. ^c Determined by GC analysis. [Pd cont. = palladium content, Conv. = conversion, and Sel. = selectivity].

observed that at a reaction time of 2 h, the catalyst showed a maximum conversion of 98% (Table 3, entry 3) with 90% selectivity for 4-CAN. On decreasing the reaction time the conversion decreases (entries 2 and 1). A maximum selectivity of 100% was achieved when the reaction was continued for 30 min with a conversion of 90% (entry 1).

Likewise, varying the Pd loading on the support from 0.84 to 1.65 wt% led to a direct decrease in conversion as well as selectivity (entry 5). Furthermore, on increasing the catalyst:substrate ratio, decreases in conversion as well as selectivity were observed (entry 4). From this screening, it was amply clear that with increase in reaction time, palladium mole content and catalyst:substrate ratio, there is always a noticeable decrease in both conversion as well as selectivity. This is understandably due to the increase in the extent of concomitant hydrodechlorination of the preformed 4-CAN.

As anticipated, lesser duration (entry 1) afforded significantly reduced formations of undesired aniline from 4-CAN by C–Cl bond scission. The temperature optimisation studies using Pd-DPPE@SiO₂ revealed that the reaction is largely temperature dependent (Fig. 7a). With increase in temperature, both conversion and selectivity for 4-CAN increase up to a temperature of 50 °C and, thereafter, they gradually decrease owing to high rates of hydrodechlorination. To understand the effect of H₂ pressure on hydrogenation of 4-CNB to the corresponding amine, the reaction was carried out at varying hydrogen pressures (Fig. 7b). The conversion increased sharply from 2 bar H₂ (60%) and attained completion at 12 bar H₂. The selectivity was marked by a steady increase from 2 bar H₂ (58%) to 8 bar H₂ (66%)

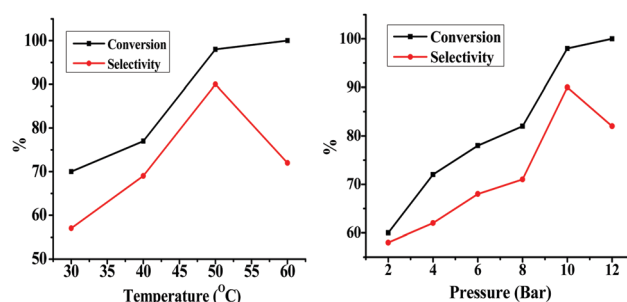


Fig. 7 Plots of temperature (left) and H₂ pressure (right) optimization studies for the Pd-DPPE@SiO₂ catalyst (0.02 mmol) with 4-CNB as the model substrate (0.5 mmol) and ethanol (4.5 mL) as the solvent for 2 hours.

Table 4 Hydrogenation of nitroarenes to aromatic amines with Pd-DPPE@SiO₂ as catalyst under liquid phase conditions^a

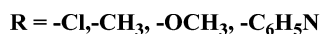
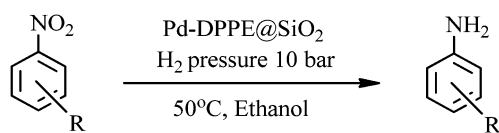
Entry	Substrate	Product	Time (h)	Conv. ^b [%]	Sel. ^b [%]
1			0.5	85	100
2			2	90	83
3			2	98 (fresh), 80 (1st cycle), 78 (2nd cycle), 74 (3rd cycle)	90 (fresh), 78 (1st cycle), 72 (2nd cycle), 70 (3rd cycle)
4			2	74	100
5			2	90	98
6			2	69	100

^a Reaction conditions: substrate (0.5 mmol), solvent (4.5 mL), H₂ pressure (10 bar), catalyst (50 mg), 400 rpm, and 50 °C. ^b Determined by GC analysis. [Conv. = conversion, and Sel. = selectivity].

followed by a steep rise observed at 10 bar H₂ corresponding to a maximum selectivity of 90%. As anticipated, the selectivity for 4-CAN decreased significantly after reaching the maximum of 10 bar H₂. This is because of undesired hydrodechlorination which begins to predominate after 10 bar H₂. Hence, after careful investigation of a wide range of experimental parameters, a reaction temperature of 50 °C coupled with a H₂ pressure of 10 bar seemed best suited for further systematic optimization (Table 4).

The liquid phase hydrogenation of different nitroarenes to amines (Scheme 2) was carried out under the optimized conditions of 10 bar H₂ and 50 °C and the results are presented in Table 4. It was observed that both the *o*- and *m*-isomers of CNB showed similar conversions and selectivities (entries 1 and 2). Usually, substrates with electron donating groups like -CH₃ and -OCH₃ exhibited good-to-excellent conversions with excellent selectivities (entries 4 and 5). Likewise, the catalyst showed excellent selectivity for 8-nitroquinoline giving exclusively 8-aminoquinoline with moderate conversion (entry 6).

Heterogeneity of the catalyst was also checked using the hot filtration technique with 4-CNB as a substrate. The reaction was



Scheme 2 Hydrogenation of nitroarenes to corresponding amines.

performed with Pd-DPPE@SiO₂ as the catalyst under a pressure of 10 bar H₂ and temperature of 50 °C for a period of 15 minutes. The catalyst was separated from the reaction mixture and the products were analyzed using GC which exhibited a yield of 47%. The filtrate was further allowed to react for an hour under the same reaction conditions, which eventually showed no increase in product yield. This indicates that the Pd NPs were well intact in the silica matrix. The ICP-AES analysis for the sample after the third cycle exhibited a negligible loss (0.02%) in content of Pd.

Recyclability tests were performed for all the catalysts and the results are demonstrated in Fig. 9. Gradual loss in activity and selectivity were observed on subsequent recycling for all the catalysts. Compared to the catalysts, Pd-AP@SiO₂ and Pd-MP@SiO₂, the loss became more prominent in the case of Pd-DPPE@SiO₂, particularly in the first recycle. The decrease in the reactivity after the first recycle may be due to the blockage of some of the active pore sites. The morphology of the catalyst after the fourth cycle was examined using TEM (Fig. 8). The micrograph showed that the Pd NPs remained intact within the silica matrix maintaining their homogeneity without any agglomeration and exhibiting good size distribution like the fresh one; thus indicating that the catalyst can be used for still more catalytic runs. Strategically speaking, the materials Pd-AP@SiO₂ and Pd-MP@SiO₂ do not stand out as possible catalysts for the said reaction due to incompetence in either conversion or selectivity. On the other hand, Pd-DPPE@SiO₂ exhibits superior catalytic results on both grounds, thereby making it the ideal candidate for liquid-phase nitroarene hydrogenation (Fig. 9).

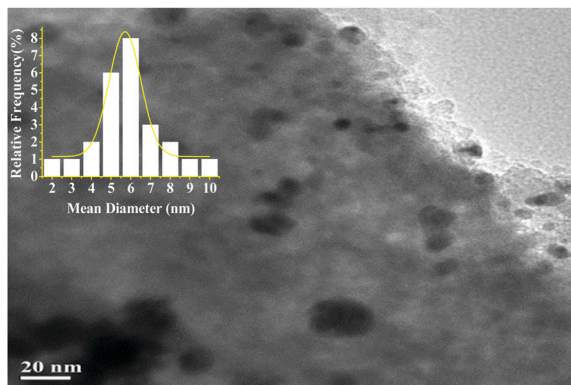


Fig. 8 TEM image of Pd-DPPE@SiO₂ after the 4th run with the corresponding size histogram (inset).

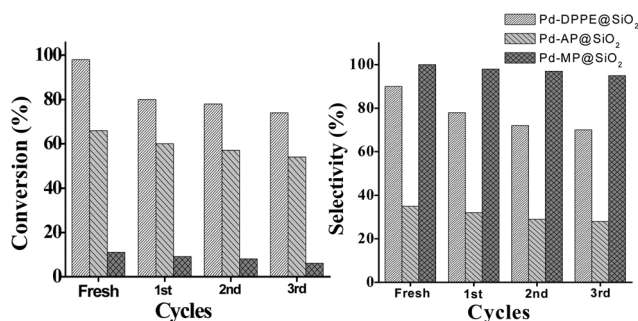


Fig. 9 Recyclability tests for the Pd NPs corresponding to both conversion and selectivity.

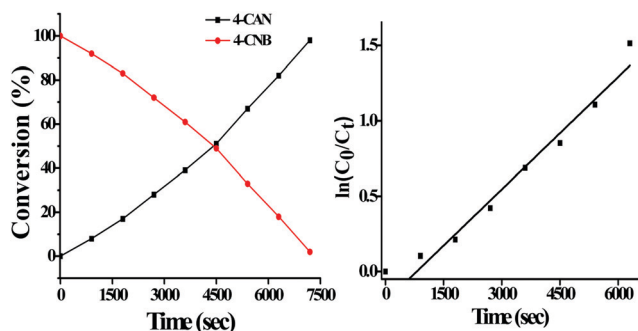


Fig. 10 Conversion vs. time curves for formation of 4-CAN from 4-CNB (left) and plot of $\ln(C_0/C_t)$ vs. time (right) catalysed by Pd-DPPE@SiO₂.

The kinetic study for conversion of 4-CNB to 4-CAN by Pd-DPPE@SiO₂ was carried out by monitoring the reaction for different time intervals and a plot of conversion *versus* time is given in Fig. 10 which follows a parabolic curve. A linear fit of pseudo-first order was observed as is evidenced from the plot of $\ln(C_0/C_t)$ *versus* time, where C_0 and C_t are the concentrations of 4-CNB at time 0 and t , respectively. From the slope of the plot, the rate constant was calculated and found to be $2.486 \times 10^{-4} \text{ s}^{-1}$. As stated earlier, there are several reports on hydrogenation of 4-CNB to 4-CAN; however, few reports exist with regards to heterogeneous Pd NP-based catalysts with molecular H₂ as a reducing agent; and, to understand the actual standing of our catalyst with respect to the reported ones we have performed a literature survey (Table 5). We are delighted to see that our catalyst is much more superior in comparison to other reported catalysts [entry 1 *vs.* entries (2–6)].

Conclusion

In summary, we have presented a facile one step protocol for synthesising Pd NPs supported on three donor ligand-functionalized silica gels and investigated their potential as catalysts for selective hydrogenation of nitroarenes. The influences of the donor ligands on the structural morphology and catalytic properties were distinctly visible. Among the three ligands, the phosphine-based catalyst, Pd-DPPE@SiO₂, was the most active and demonstrated excellent activity (98%) and selectivity (100%). Our catalyst could be easily recovered from the reaction mixture by simple filtration and recycled up to four times without compromising much with the activity and selectivity.

Experimental

Materials and method

2-Diphenylphosphinoethyl-functionalized silica gel (DPPE@SiO₂; 0.7 mmol g⁻¹ loading; 200–400 US mesh), 3-aminopropyl-functionalized silica gel (AP@SiO₂; 1 mmol g⁻¹ loading; 200–400 US mesh), 3-mercaptopropyl-functionalized silica gel, (MP@SiO₂; 1.2 mmol g⁻¹ loading; 200–400 US mesh) and PdCl₂ were purchased from Sigma-Aldrich. All solvents, substrates and other chemicals were purchased from Acros Organics (purity >98%) and Merck (purity >99%). PXRD analysis were carried out in an Ultima IV Powder X-ray diffractometer using

Table 5 Hydrogenation of 4-CNB to 4-CAN with Pd-DPPE@SiO₂ as catalyst under liquid phase conditions^a

Catalyst	Catalyst (w/w%) ^b	Conditions	Conv.	Prod. (s) (Sel. %) ^c	Ref.
Pd-DPPE@SiO ₂	0.84	50 °C, 10 bar, 30 min	90	4-CAN (100)	Present work ^d
Pd/Al ₂ O ₃	0.35	100 °C, 11 bar, —	100	AN (56), NB (44)	11
Pd/Al ₂ O ₃	1.2	100 °C, 1 bar, —	100	AN (52), NB (48)	47
Pd/ZnO	4.7	180 °C, 1 bar, 180 min	92	4-CAN (95.9) AN (4)	32
Pd/-Fe ₂ O ₃ -PR	3	80 °C, 10–40 bar, 300 min	100	4-CAN (96.2), NB (3.1)	36
Pd/C	2	100 °C, 1 bar, 115 min	100	4-CAN (95.92), AN (4.08)	34

^a Reaction conditions: substrate (0.5 mmol), solvent (4.5 mL), H₂ pressure (10 bar), catalyst (50 mg), 400 rpm, 50 °C, and 2 h. ^b Metal content of the Pd NPs as measured from ICP-AES analysis. ^c Determined by GC analysis; 4CAN = 4chloronitrobenzene; AN = aniline; NB = nitrobenzene. [Conv. = conversion, Prod. = product, Sel. = selectivity, Ref. = references].

CuK α as source ($\lambda = 1.54 \text{ \AA}$) with a scan rate of $2\theta = 4^\circ \text{ min}^{-1}$. X-ray photoelectron spectroscopy (XPS) analysis was carried out using a FEI PHI 5000 Versa Prob II system. The thermogravimetric measurements were carried out using a Perkin Elmer TGA-DTA analyzer (Model: STA 8000) taking $\alpha\text{-Al}_2\text{O}_3$ as the reference sample. Samples weighing 5.0 mg were heated from 35 to 800 °C under nitrogen atmosphere at a rate of $20^\circ \text{ C min}^{-1}$. Surface area measurements were carried out at liquid nitrogen temperature in a Quantachrome Autosorb-iQ analyser using N_2 gas as adsorbent. Surface area calculations were carried out from the isotherm using the BET model and pore size distributions were calculated using the BJH model. Samples were degassed at 100 °C for 2 h before performing the experiment. Transmission electron microscopy (TEM) images were recorded in a JEOL, JEM-2100 transmission electron microscope with an accelerating voltage of 200 keV. The ICP-AES analysis was performed in an ACROS simultaneous ICP spectrometer equipped with an R. F. generator (1.6 KW, 27.12 MHz), with wavelengths in the range of 130–770 nm. The hydrogenation reactions were carried out in a reactor made of Hastelloy (model: 5500, make: Parr Instruments, USA). Gas chromatographic analysis of the reactants and products was performed in a Perkin Elmer Clarus 480 GC system equipped with a capillary column (L 30 m, I.D. 0.25 mm) fitted with an FID.

Synthesis of Na_2PdCl_4

The Pd precursor was synthesized by adding PdCl_2 to a solution of NaCl in water and stirred for 1 h to yield the desired Na_2PdCl_4 solution.⁴⁸

Synthesis of Pd-DPPE@SiO_2 , Pd-AP@SiO_2 and Pd-MP@SiO_2

2.0 g of Pd-DPPE@SiO_2 was taken in a 100 mL round bottom flask containing 20 mL distilled water and stirred for 30 minutes to achieve complete dispersion. To the resultant mixture, 20 mL of 0.01 mmol Na_2PdCl_4 solution was added and stirred for an hour. The colour of the silica gel changed to bright yellow. To it 4 mL (51.2% V/V) hydrazine solution was added drop wise over a period of 15 minutes and the colour instantly changed to light brown. The stirring was continued for 1 h to ensure complete reduction of Na_2PdCl_4 . The resultant solid mass was filtered and washed several times with small aliquots of distilled water followed by drying at room temperature and kept in a desiccator. Two more samples were prepared by varying the palladium content. Following the same procedure, Pd-AP@SiO_2 and Pd-MP@SiO_2 materials were also synthesized on AP@SiO_2 and MP@SiO_2 respectively.

General procedure for catalytic hydrogenation

The catalytic hydrogenation reaction of aromatic nitroarenes to corresponding amines was carried out by charging 0.5 mmol of nitroarenes in 4.5 mL ethanol into an autoclave reactor made of Hastelloy. 50 mg of catalyst was added to the reaction mixture and the autoclave was initially purged with hydrogen gas for 5 minutes and then pressurized to 10 bar at room temperature. The reactor vessel was heated to 50 °C with constant stirring (550 rpm) for the desired period. After completion of the reaction,

the reactor vessel was cooled to room temperature and depressurized. The reaction mixture was separated from the catalyst by simple filtration and analyzed using GC.

General procedure for recyclability tests

The catalysts for the recyclability tests were recovered from the reaction mixture after fresh runs by simple filtration followed by washing and drying. All the recyclability tests were performed maintaining the same stoichiometric ratios.

Conflicts of interest

There are no conflicts to declare.

Acknowledgements

DST, New Delhi is gratefully acknowledged for financial support (Project No: EMR/2015/000021). The UGC, New Delhi is also acknowledged for the SAP-DRS-I grant to the Department of Chemistry, Dibrugarh University. CSIR-IIP, Dehradun and IIT, Kanpur are greatly acknowledged for various analytical services.

Notes and references

- 1 A. M. Tafesh and J. Weiguny, *Chem. Rev.*, 1996, **96**, 2035–2052.
- 2 D. A. Boehncke, J. Kielhorn and I. Mangelsdorf, *4-CHLOROANILINE-Concise International Chemical Assessment Document (CICAD)*, WHO, 2003.
- 3 H. H. Baer, R. G. Coombes, P. C. Myhre and A. T. Nielsen, *The Nitro Group in Organic Synthesis*, Wiley-VCH, 2001.
- 4 H. Blaser, H. Steiner and M. Studer, *ChemCatChem*, 2009, **1**, 210–221.
- 5 T. Kletz, P. L. Spargo, M. Place and S. Cross, *Org. Process Res. Dev.*, 2005, **9**, 1015–1025.
- 6 H. van Bekkum and R. A. Sheldon, *Fine Chemicals through Heterogeneous Catalysis*, Wiley-VCH, 2001.
- 7 H. Blaser, C. Malan, B. Pugin, F. Spindler and M. Studer, *Adv. Synth. Catal.*, 2003, **345**, 103–151.
- 8 E. G. Ertl, H. Kniizinger, J. Weitkamp, A. Part, K. S. Suslick and S. M. Ave, *Handbook of Heterogeneous Catalysis*, 1997.
- 9 G. Wienh, A. Boddien, F. Westerhaus, K. Junge, H. Junge, R. Llusar and M. Beller, *J. Am. Chem. Soc.*, 2011, **133**, 12875–12879.
- 10 A. Corma, P. Serna, P. Concepción and J. J. Calvino, *J. Am. Chem. Soc.*, 2008, **130**, 8748–8753.
- 11 F. Cárdenas-lizana, S. Gómez-quero, A. Hugon, L. Delannoy, C. Louis and M. A. Keane, *J. Catal.*, 2009, **262**, 235–243.
- 12 A. H. Pizarro, C. B. Molina, J. A. Casas and J. J. Rodriguez, *Appl. Catal., B*, 2014, **158–159**, 175–181.
- 13 W. Jia, S. Ling, H. Zhang, E. Sheng and R. Lee, *Organometallics*, 2018, **37**, 1–8.
- 14 W. J. Kerr, R. J. Mudd and J. A. Brown, *Chem. – Eur. J.*, 2016, **3**, 4738–4742.
- 15 S. Fountoulaki, V. Daikopoulou, P. L. Gkizis, I. Tamiolakis, G. S. Armatas and I. N. Lykakis, *ACS Catal.*, 2014, **4**, 3504–3511.

- 16 M. Oubenali, G. Vanucci, B. Machado, M. Kacimi, M. Ziyad, J. Faria, A. Raspolli-galetti and P. Serp, *ChemSusChem*, 2011, **4**, 950–956.
- 17 H. Yang, X. Cui, Y. Deng and F. Shi, *ChemCatChem*, 2013, **5**, 1–5.
- 18 D. He, X. Jiao, P. Jiang and B. Xu, *Green Chem.*, 2012, **14**, 111–116.
- 19 D. He, H. Shi, Y. Wu and B. Xu, *Green Chem.*, 2007, **9**, 849–851.
- 20 G. Bai, Z. Zhao, H. Dong, L. Niu, Y. Wang and Q. Chen, *ChemCatChem*, 2014, **6**, 655–662.
- 21 M. Makosch, J. Su, C. Kartusch, G. Richner and J. A. Van Bokhoven, *ChemCatChem*, 2012, **4**, 59–63.
- 22 N. Maity, P. R. Rajamohanan, S. Ganapathy, C. S. Gopinath, S. Bhaduri and G. K. Lahiri, *J. Phys. Chem. C*, 2008, **112**, 9428–9433.
- 23 X. Wang, J. J. Delgado, G. Blanco, X. Chen and C. M. Olmos, *J. Phys. Chem. C*, 2013, **117**, 994–1005.
- 24 K. Shimizu, Y. Miyamoto, T. Kawasaki, T. Tanji, Y. Tai and A. Satsuma, *J. Phys. Chem. C*, 2009, **113**, 17803–17810.
- 25 H. Shin and S. Huh, *ACS Appl. Mater. Interfaces*, 2012, **4**, 6324–6331.
- 26 D. M. Dotzauer, S. Bhattacharjee, Y. Wen and M. L. Bruening, *Langmuir*, 2009, **25**, 1865–1871.
- 27 H. Jiang, T. Akita, T. Ishida, M. Haruta and Q. Xu, *J. Am. Chem. Soc.*, 2011, **133**, 1304–1306.
- 28 S. Park, I. S. Lee and J. Park, *Org. Biomol. Chem.*, 2013, **11**, 395–399.
- 29 H. Huang, X. Wang, M. Tan, C. Chen and X. Zou, *ChemCatChem*, 2016, **8**, 1485–1489.
- 30 E. Bertolucci, R. Bacsá, A. Benyounes, A. M. Raspolli-Galletti, M. R. Axet and P. Serp, *ChemCatChem*, 2015, **7**, 2971–2978.
- 31 J. Lyu, J. Wang, C. Lu, Q. Zhang, X. He and X. Li, *J. Phys. Chem. C*, 2014, **115**, 2594–2601.
- 32 Y. Hao, M. Crespo-quesada, I. Yuranov, X. Wang, M. A. Keane and L. Kiwi-minsker, *ACS Catal.*, 2013, **3**, 1386–1396.
- 33 E. Bertolucci, R. Bacsá, A. Benyounes, A. M. Raspolli-Galletti, M. R. Axet and P. Serp, *ChemCatChem*, 2015, **7**, 2971–2978.
- 34 S. Jayakumar, A. Modak, M. Guo, H. Li and X. Hu, *Chem. – Eur. J.*, 2017, **23**, 7791–7797.
- 35 Y. Guari, C. Thieuleux, A. Mehdi, C. Reye, R. J. P. Corriu, S. Gomez-Gallardo, K. Philippot, B. Chaudret and R. Dutartre, *Chem. Commun.*, 2001, 1374–1375.
- 36 A. B. Hungria, R. Raja, R. D. Adams, B. Captain, J. M. Thomas, P. A. Midgley, V. Golovko and B. F. G. Johnson, *Angew. Chem., Int. Ed.*, 2006, **47**, 4782–4785.
- 37 R. Xing, Y. Liu, H. Wu, X. Li, M. He and P. Wu, *Chem. Commun.*, 2008, 6297–6299.
- 38 Z. Hou, N. Theyssen, A. Brinkmann, K. V. Klementiev, W. Grünert, M. Bühl, W. Schmidt, B. Spliethoff, B. Tesche and C. Weidenthaler, *J. Catal.*, 2008, **258**, 315–323.
- 39 B. Karimi, S. Abedi, J. H. Clark and V. Budarin, *Angew. Chem., Int. Ed.*, 2006, **45**, 4776–4779.
- 40 F. P. da Silva, J. L. Fiorio and L. M. Rossi, *ACS Omega*, 2017, **2**, 6014–6022.
- 41 N. J. S. Costa and L. M. Rossi, *Nanoscale*, 2012, **4**, 5826–5834.
- 42 L. M. Rossi, I. M. Nangoi and J. S. Costa, *Inorg. Chem.*, 2009, **48**, 4640–4642.
- 43 L. M. Rossi, F. P. Silva, L. L. R. Vono, P. K. Kiyohara and E. L. Duarte, *Green Chem.*, 2007, **9**, 379–385.
- 44 N. Almora-barrios, R. Verel and J. Pérez-Ramírez, *Catal. Sci. Technol.*, 2015, **6**, 1621–1631.
- 45 D. Sahu and P. Das, *RSC Adv.*, 2014, **5**, 3512–3520.
- 46 L. M. Rossi, J. L. Fiorio, M. A. S. Garcia and C. P. Ferraz, *Dalton Trans.*, 2018, **47**, 5889–5915.
- 47 X. Wang, N. Perret and M. A. Keane, *Chem. Eng. J.*, 2012, **210**, 103–113.
- 48 T. Teranishi and M. Miyake, *Chem. Mater.*, 1998, **4756**, 594–596.